science.sciencemag.org/cgi/content/full/science.aau6103/DC1

Supplementary Materials for

Synthetic dissipation and cascade fluxes in a turbulent quantum gas

Nir Navon*, Christoph Eigen, Jinyi Zhang, Raphael Lopes, Alexander L. Gaunt,
Kazuya Fujimoto*, Makoto Tsubota, Robert P. Smith, Zoran Hadzibabic

*Corresponding author. Email: nir.navon@yale.edu (N.N.); kazuya_fujimoto@rover.nuap.nagoya-u.ac.jp (K.F.)

Published 3 October 2019 on *Science* First Release
DOI: 10.1126/science.aau6103

This PDF file includes:

Supplementary Text
Figs. S1 to S3
References and Notes

Calibration of the shaking force and the resonant driving frequency

The shaking force is produced by coils that create a magnetic field gradient. We calibrate its magnitude F (for a given voltage applied to the coils) by switching off the box trap, immediately pulsing the force for a time δt, and measuring the resulting velocity kick $\delta v = F\delta t/m$; to determine δv we measure the position of the cloud's centre of mass, x_{CoM}, after a time of flight t_{ToF}.

Due to the optical resolution of the system used to create the box trap, the trap walls are not perfectly sharp [26], and consequently the frequency of the lowest axial sound mode, ω_{res}, slightly depends on U_{D}. To ensure that the gas is always driven on resonance, we measure $\omega_{\mathrm{res}}(U_{\mathrm{D}})$. We perform stroboscopic modulation spectroscopy by applying the driving force $F_0 \sin(\omega_{\mathrm{s}} t)$ for $t_{\mathrm{s}} = 2$ s, with $F_0 L \approx k_{\mathrm{B}} \times 2.5$ nK, and then releasing the cloud and measuring x_{CoM} after $t_{\mathrm{ToF}} = 140$ ms. Choosing discrete values of ω_{s} such that $\omega_{\mathrm{s}} t_{\mathrm{s}} = 2\pi j + \pi/2$, where j is an integer, the resulting x_{CoM} has an absorptive shape and we fit it with the function

$$x_{\mathrm{CoM}} \propto \frac{\omega_{\mathrm{s}}^2}{(\omega_{\mathrm{s}}^2 - \omega_{\mathrm{res}}^2)^2 + \Gamma^2 \omega_{\mathrm{s}}^2}\,, \tag{S1}$$

where Γ is the linewidth. In Fig. S1 we show such line shapes for two different U_{D}, and the plot of ω_{res} versus U_{D}.

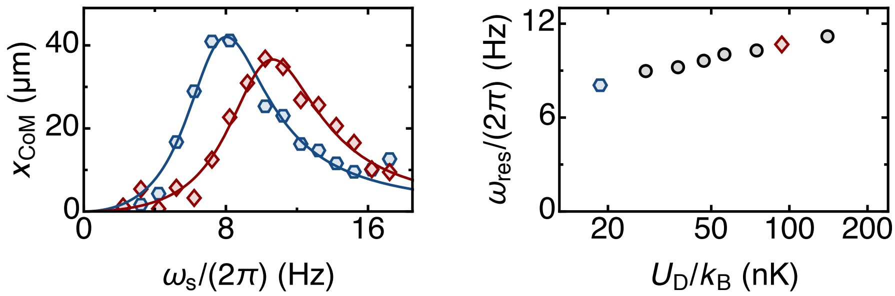

Figure S1: **The resonant drive frequency.** Left: Resonance measurements for $U_{\mathrm{D}}/k_{\mathrm{B}} = 19$ nK (blue) and 94 nK (red); solid lines are fits based on Eq. (S1). Right: ω_{res} versus U_{D}.

Numerical simulations

Gross-Pitaevskii simulations with dissipation

The starting point for our simulations is the Gross-Pitaevskii equation (GPE) for the classical field $\psi(\mathbf{r}, t)$:

$$i\hbar \frac{\partial \psi}{\partial t} = \left(-\frac{\hbar^2}{2m} \nabla^2 + V(\mathbf{r}, t) + g|\psi|^2 \right) \psi\,, \tag{S2}$$

where $g = 4\pi\hbar^2 a_s/m$ and a_s is the s-wave scattering length. If $V(\mathbf{r}, t) \in \mathbb{R}$, the evolution of the GPE conserves the total particle number $N = \int |\psi|^2\,\mathrm{d}\mathbf{r}$. Introducing dissipation in the GPE is a subtle problem [41-44]. We introduce a phenomenological term in $V(\mathbf{r}, t)$ that closely resembles the dissipation process in our experiment. We write:

$$V(\mathbf{r}, t) = V_{\mathrm{box}}(\mathbf{r}) + V_{\mathrm{osc}}(\mathbf{r}, t) - iV_{\mathrm{diss}}(\mathbf{r}),$$

where V_{box} is the box potential, V_{osc} is the forcing potential, and iV_{diss} is an imaginary 'sponge' potential that 'absorbs' particles with sufficiently high energy to leave the trap and removes them from the system. More precisely:

$$V_{\mathrm{box}}(\mathbf{r}) = \begin{cases} 0 & \text{if } |x| \leq \frac{L}{2},\ \sqrt{y^2 + z^2} \leq R \\ U_{\mathrm{D}} & \text{otherwise}\,, \end{cases}$$

$$V_{\mathrm{osc}}(\mathbf{r}, t) = Fx \sin(\omega_{\mathrm{res}} t)\,,$$

and

$$V_{\mathrm{diss}}(\mathbf{r}) = \begin{cases} 0 & \text{if } |x| \leq \frac{L+2\delta}{2},\ \sqrt{y^2 + z^2} \leq R + \delta \\ V_{\mathrm{D}} & \text{otherwise}\,. \end{cases}$$

The phenomenological parameter δ, the spatial offset between the edge of the box and the sponge, is introduced because even if all particles are trapped, for a non-infinite $U_{\rm D}$ an evanescent component of $\psi(\mathbf{r},t)$ exists outside the box. We have verified that for a wide range of $V_{\rm D}$ and δ our results do not depend on their exact values (see Fig. S2 below).

We numerically solve Eq. (S2) using a pseudo-spectral method with the fourth-order Runge-Kutta time evolution. In simulations $L = 27$ µm, $R = 16$ µm, and the initial atom number is $N_0 = 1.2\times10^5$, corresponding to chemical potential $\mu = gn_0 = k_{\rm B}\times 2.0$ nK, where $n_0 = N_0/(\pi R^2 L)$. The size of our whole numerical grid is $40\,\xi\times40\,\xi\times40\,\xi$, where $\xi = \hbar/\sqrt{2mgn_0} = 1.2$ µm is the healing length. The spatial and temporal resolutions are $\frac{40}{128}\xi$ and $10^{-3}\hbar/\mu = 3.7$ µs respectively.

The initial $\psi(\mathbf{r},t=0)$ is determined by calculating the ground state in the static trap ($F = 0$ and $V_{\rm D} = 0$), using imaginary-time evolution of the GPE. The resonant driving frequency $\omega_{\rm res}$ is then determined by numerically solving the Bogoliubov equations on $\psi(\mathbf{r},0)$. For all experimentally explored $U_{\rm D}$ we get $\omega_{\rm res}\approx 2\pi\times 8.8$ Hz, with variations of $< 3\%$. Finally, to simulate the shaking experiments, we solve the real-time GPE with the forcing amplitude $F = F_0 = 1.22\ \mu/L$ and nonzero $V_{\rm D}$. Our results are based on a single run using the same deterministic initial condition $\psi(\mathbf{r},0)$.

Atom-loss dynamics

In Fig. S2 we show simulated atom loss $N_0 - N(t_{\rm s})$, where $N(t_{\rm s}) = \int|\psi(\mathbf{r},t_{\rm s})|^2\,\mathbf{dr}$, for $U_{\rm D} = k_{\rm B}\times 25$ nK and various combinations of the dissipation parameters $V_{\rm D}$ and δ. In all cases we see curves similar to the experimental ones shown in Fig. 2 in the main paper (and for the results shown in the main paper we analyze them in the same way as the experimental data). For a fixed $V_{\rm D} = 5\mu$, we get essentially indistinguishable results for any $\delta \gtrsim 7/k_{\rm D}$. Qualitatively, δ needs to be sufficiently larger than $1/k_{\rm D}$ for the probability of absorbing (on a timescale $t_{\rm s}$) particles with energies below $U_{\rm D}$ to be vanishingly small; otherwise we remove too many particles. For a fixed $\delta = 10.5/k_{\rm D}$ we get essentially the same results for any $V_{\rm D}\gtrsim\mu$.

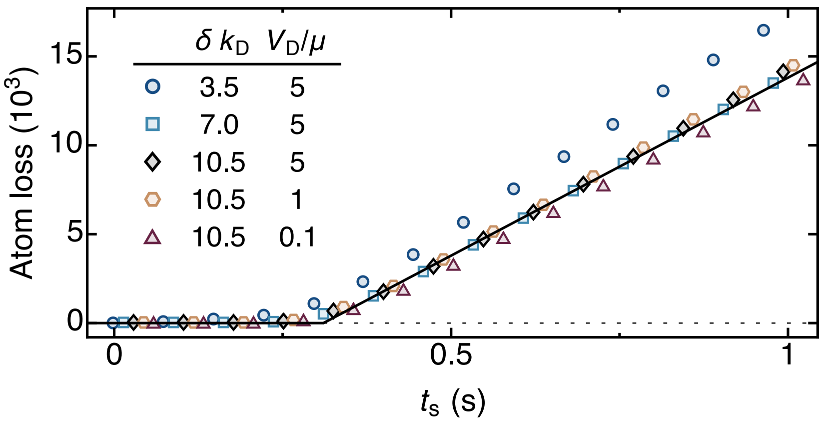

Figure S2: **Atom-loss dynamics in numerical simulations.** Atoms lost versus shaking time for $U_{\rm D} = k_{\rm B}\times 25$ nK and various combinations of the dissipation parameters $V_{\rm D}$ and δ. The solid black line is a piece-wise linear fit to the numerical data for $\delta = 10.5/k_{\rm D}$ and $V_{\rm D} = 5\mu$, from which t_d and Π_n are extracted (see main text). For clarity only a subset of $t_{\rm s}$ values are plotted.

Fourier-space dynamics

We also compute the evolution of the momentum distribution in the presence of shaking and dissipation, supporting the qualitative picture outlined in Fig. 4A in the main paper. The momentum distributions are averaged over spherical shells to obtain $n(k)$, and normalised such that $\sum_k 4\pi k^2 n(k)\delta k = N$, where $\delta k = \frac{\pi}{20\xi}$ is the grid resolution in $\mathbf{k}$ space. In Fig. S3A, we show $n(k)$ for $U_{\rm D} = k_{\rm B}\times 130$ nK and various shaking times $t_{\rm s}$. The power-law distribution $n(k)\sim k^{-\gamma}$ (with $\gamma\approx 3.5$) develops in the wake of the cascade front, and as the cascade front propagates with $k_{\rm cf}(t_{\rm s})\propto t_{\rm s}^{1/(2\beta)}$ the momentum distribution $n(k)$ evolves in a self-similar way. As shown in Fig. S3B, this self-similarity is revealed by the collapse of the curves shown in Fig. S3A for $t\lesssim t_{\rm d}$ when plotting $n(k,t_{\rm s})$ in the rescaled form $(t_{\rm s}/t_{\rm ref})^a n((t_{\rm s}/t_{\rm ref})^{-b}k,t_{\rm s})$, with $b = 1/(2\beta) = 1/(5-\gamma) = 0.67$, $a = b\gamma = 2.33$, and setting arbitrarily $t_{\rm ref} = 1$s. Note that the successful collapse of the curves for these values of a and b also confirms our assumption that the energy input rate is time independent. Once the cascade front reaches the dissipation scale $k_{\rm D}$ (for $t_{\rm s} > t_{\rm d}$) a steady state is established over the entire inertial range.

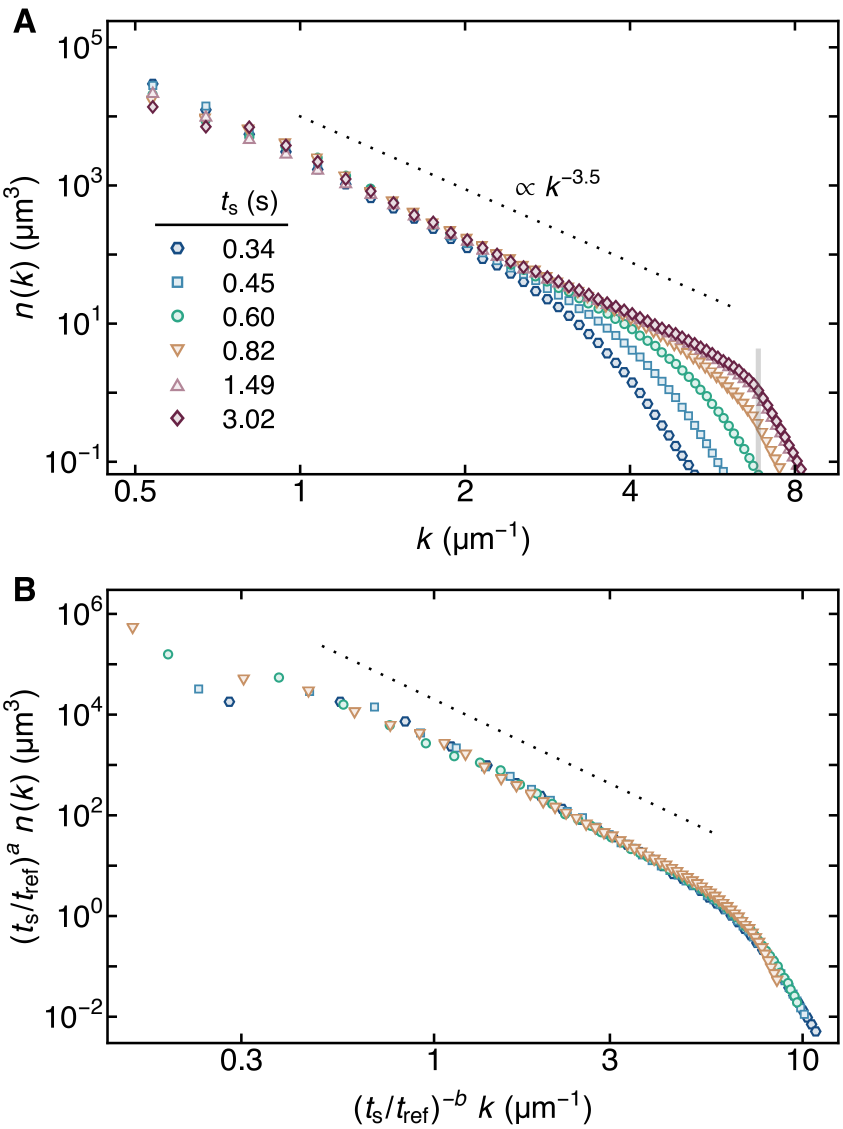

Figure S3: **Momentum-space dynamics in numerical simulations.** (**A**) $n(k)$ computed for $U_D = k_B \times 130$ nK and various shaking times t_s. The power-law momentum distribution $n(k) \sim k^{-\gamma}$, with $\gamma \approx 3.5$, develops in the wake of the cascade front. A steady state is established once the cascade front reaches k_D; in this example $k_D = 8/\xi$, indicated by the vertical grey band. (**B**) The momentum distributions from (**A**) with $t_s \lesssim t_d \approx 1.0$ s rescaled with $a = \gamma/(5-\gamma) = 2.33$, $b = 1/(5-\gamma) = 0.67$, and $t_{ref} = 1$ s (see text) collapse onto a single curve, indicating self-similar behavior.

References and Notes

1. A. N. Kolmogorov, The local structure of turbulence in an incompressible viscous fluid at very high Reynolds numbers. *Dokl. Akad. Nauk SSSR* **30**, 299–303 (1941).
2. A. Obukhov, On the distribution of energy in the spectrum of turbulent flow. *Dokl. Akad. Nauk SSSR* **32**, 22–24 (1941).
3. V. E. Zakharov, V. S. L'vov, G. Falkovich, *Kolmogorov Spectra of Turbulence* (Springer, 1992).
4. S. Dyachenko, A. Newell, A. Pushkarev, V. Zakharov, Optical turbulence: Weak turbulence, condensates and collapsing filaments in the nonlinear Schrödinger equation. *Physica D* **57**, 96–160 (1992). doi:10.1016/0167-2789(92)90090-A
5. U. Frisch, *Turbulence: The Legacy of A. N. Kolmogorov* (Cambridge Univ. Press, 1995).
6. O. Alexandrova, J. Saur, C. Lacombe, A. Mangeney, J. Mitchell, S. J. Schwartz, P. Robert, Universality of solar-wind turbulent spectrum from MHD to electron scales. *Phys. Rev. Lett.* **103**, 165003 (2009). doi:10.1103/PhysRevLett.103.165003 Medline
7. J. Salort, C. Baudet, B. Castaing, B. Chabaud, F. Daviaud, T. Didelot, P. Diribarne, B. Dubrulle, Y. Gagne, F. Gauthier, A. Girard, B. Hébral, B. Rousset, P. Thibault, P.-E. Roche, Turbulent velocity spectra in superfluid flows. *Phys. Fluids* **22**, 125102 (2010). doi:10.1063/1.3504375
8. A. Chepurnov, B. Burkhart, A. Lazarian, S. Stanimirovic, The turbulence velocity power spectrum of neutral hydrogen in the Small Magellanic Cloud. *Astron. J.* **810**, 33 (2015). doi:10.1088/0004-637X/810/1/33
9. N. Navon, A. L. Gaunt, R. P. Smith, Z. Hadzibabic, Emergence of a turbulent cascade in a quantum gas. *Nature* **539**, 72–75 (2016). doi:10.1038/nature20114 Medline
10. W. D. McComb, *Homogeneous, Isotropic Turbulence: Phenomenology, Renormalization and Statistical Closures* (Oxford Univ. Press, 2014).
11. M. S. Uberoi, Energy Transfer in Isotropic Turbulence. *Phys. Fluids* **6**, 1048 (1963). doi:10.1063/1.1706861
12. M. Miyake, M. Donelan, Y. Mitsuta, Airborne measurement of turbulent fluxes. *J. Geophys. Res.* **75**, 4506–4518 (1970). doi:10.1029/JC075i024p04506
13. L. Deike, M. Berhanu, E. Falcon, Energy flux measurement from the dissipated energy in capillary wave turbulence. *Phys. Rev. E* **89**, 023003 (2014). doi:10.1103/PhysRevE.89.023003 Medline

14. E. A. L. Henn, J. A. Seman, G. Roati, K. M. F. Magalhães, V. S. Bagnato, Emergence of turbulence in an oscillating Bose-Einstein condensate. *Phys. Rev. Lett.* **103**, 045301 (2009). doi:10.1103/PhysRevLett.103.045301 Medline

15. T. W. Neely, A. S. Bradley, E. C. Samson, S. J. Rooney, E. M. Wright, K. J. H. Law, R. Carretero-González, P. G. Kevrekidis, M. J. Davis, B. P. Anderson, Characteristics of two-dimensional quantum turbulence in a compressible superfluid. *Phys. Rev. Lett.* **111**, 235301 (2013). doi:10.1103/PhysRevLett.111.235301 Medline

16. W. J. Kwon, G. Moon, J. Choi, S. W. Seo, Y. Shin, Relaxation of superfluid turbulence in highly oblate Bose-Einstein condensates. *Phys. Rev. A* **90**, 063627 (2014). doi:10.1103/PhysRevA.90.063627

17. M. C. Tsatsos, P. E. S. Tavares, A. Cidrim, A. R. Fritsch, M. A. Caracanhas, F. E. A. dos Santos, C. F. Barenghi, V. S. Bagnato, Quantum turbulence in trapped atomic Bose-Einstein condensates. *Phys. Rep.* **622**, 1–52 (2016). doi:10.1016/j.physrep.2016.02.003

18. W. J. Kwon, J. H. Kim, S. W. Seo, Y. Shin, Observation of von Kármán Vortex Street in an Atomic Superfluid Gas. *Phys. Rev. Lett.* **117**, 245301 (2016). doi:10.1103/PhysRevLett.117.245301 Medline

19. S. W. Seo, B. Ko, J. H. Kim, Y. Shin, Observation of vortex-antivortex pairing in decaying 2D turbulence of a superfluid gas. *Sci. Rep.* **7**, 4587 (2017). doi:10.1038/s41598-017-04122-9 Medline

20. M. E. Mossman, M. A. Hoefer, K. Julien, P. G. Kevrekidis, P. Engels, Dissipative shock waves generated by a quantum-mechanical piston. *Nat. Commun.* **9**, 4665 (2018). doi:10.1038/s41467-018-07147-4 Medline

21. S. P. Johnstone, A. J. Groszek, P. T. Starkey, C. J. Billington, T. P. Simula, K. Helmerson, Evolution of large-scale flow from turbulence in a two-dimensional superfluid. *Science* **364**, 1267–1271 (2019). doi:10.1126/science.aat5793 Medline

22. G. Gauthier, M. T. Reeves, X. Yu, A. S. Bradley, M. A. Baker, T. A. Bell, H. Rubinsztein-Dunlop, M. J. Davis, T. W. Neely, Giant vortex clusters in a two-dimensional quantum fluid. *Science* **364**, 1264–1267 (2019). doi:10.1126/science.aat5718 Medline

23. B. V. Svistunov, *J. Mosc. Phys. Soc.* **1**, 373 (1991).

24. D. V. Semikoz, I. I. Tkachev II, Kinetics of Bose condensation. *Phys. Rev. Lett.* **74**, 3093–3097 (1995). doi:10.1103/PhysRevLett.74.3093 Medline

25. D. V. Semikoz, I. I. Tkachev, Condensation of bosons in the kinetic regime. *Phys. Rev. D Part. Fields* **55**, 489–502 (1997). doi:10.1103/PhysRevD.55.489

26. A. L. Gaunt, T. F. Schmidutz, I. Gotlibovych, R. P. Smith, Z. Hadzibabic, Bose-Einstein condensation of atoms in a uniform potential. *Phys. Rev. Lett.* **110**, 200406 (2013). doi:10.1103/PhysRevLett.110.200406 Medline

27. See supplementary materials.

28. The exponent $\gamma \approx 3.5$ is close to the Kolmogorov-Zakharov prediction for (compressible) weak-wave turbulence in three dimensions, $\gamma = 3$, and in agreement with numerical simulations of the Gross-Pitaevskii equation (*9*), as well as with a scaling analysis of kinetic equations (*29*).

29. I. Chantesana, A. P. Orioli, T. Gasenzer, Kinetic theory of nonthermal fixed points in a Bose gas. *Phys. Rev. A* **99**, 043620 (2019). doi:10.1103/PhysRevA.99.043620

30. O. Cadot, Y. Couder, A. Daerr, S. Douady, A. Tsinober, Energy injection in closed turbulent flows: Stirring through boundary layers versus inertial stirring. *Phys. Rev. E* **56**, 427–433 (1997). doi:10.1103/PhysRevE.56.427

31. Note that the lowest U_D we explore corresponds to $U_D/\mu \approx 10$, $U_D/(F_0L) \approx 8$ and $k_D/k_F \approx 23$.

32. Note that it is the total radial flux Π_n, rather than $|\mathbf{\Pi}_n|$, that is k-independent in the inertial range.

33. J. C. Vassilicos, Dissipation in Turbulent Flows. *Annu. Rev. Fluid Mech.* **47**, 95–114 (2015). doi:10.1146/annurev-fluid-010814-014637

34. For incompressible flows, the Kolmogorov dissipation lengthscale, analogous to our $1/k_D$, depends on the viscosity of the fluid (as $\propto \nu^{3/4}$).

35. In most familiar systems, like the damped harmonic oscillator, the rate at which the system absorbs energy in steady state depends on both the driving and the dissipation.

36. S. Nazarenko, *Wave Turbulence* (Springer, 2011).

37. M. Prüfer, P. Kunkel, H. Strobel, S. Lannig, D. Linnemann, C.-M. Schmied, J. Berges, T. Gasenzer, M. K. Oberthaler, Observation of universal dynamics in a spinor Bose gas far from equilibrium. *Nature* **563**, 217–220 (2018). doi:10.1038/s41586-018-0659-0 Medline

38. C. Eigen, J. A. P. Glidden, R. Lopes, E. A. Cornell, R. P. Smith, Z. Hadzibabic, Universal prethermal dynamics of Bose gases quenched to unitarity. *Nature* **563**, 221–224 (2018). doi:10.1038/s41586-018-0674-1 Medline

39. S. Erne, R. Bücker, T. Gasenzer, J. Berges, J. Schmiedmayer, Universal dynamics in an isolated one-dimensional Bose gas far from equilibrium. *Nature* **563**, 225–229 (2018). doi:10.1038/s41586-018-0667-0 Medline

40. N. Navon *et al*., Research data and code supporting "Synthetic dissipation and cascade fluxes in a turbulent quantum gas". Apollo (2019). 10.17863/CAM.41553

41. M. Kobayashi, M. Tsubota, Kolmogorov spectrum of superfluid turbulence: Numerical analysis of the Gross-Pitaevskii equation with a small-scale dissipation. *Phys. Rev. Lett.* **94**, 065302 (2005). doi:10.1103/PhysRevLett.94.065302 Medline

42. A. Griffin, T. Nikuni, E. Zaremba, *Bose-Condensed Gases at Finite Temperatures* (Cambridge Univ. Press, 2009).

43. D. Proment, S. Nazarenko, M. Onorato, Quantum turbulence cascades in the Gross-Pitaevskii model. *Phys. Rev. A* **80**, 051603 (2009). doi:10.1103/PhysRevA.80.051603

44. M. T. Reeves, T. P. Billam, B. P. Anderson, A. S. Bradley, Identifying a Superfluid Reynolds Number via Dynamical Similarity. *Phys. Rev. Lett.* **114**, 155302 (2015). doi:10.1103/PhysRevLett.114.155302 Medline